



Contents lists available at ScienceDirect

Biosensors and Bioelectronics

journal homepage: www.elsevier.com/locate/bios

Low-cost and sustainable smartphone-based tissue-on-chip device for bioluminescence biosensing

Maria Maddalena Calabretta^{a,b}, Denise Gregucci^{a,b}, Massimo Guardigli^a, Elisa Michelini^{a,b,c,*}

^a Department of Chemistry "Giacomo Ciamician", University of Bologna, Via P. Gobetti 85, 40129, Bologna, Italy

^b Center for Applied Biomedical Research (CRBA), Azienda Ospedaliero-Universitaria Policlinico S. Orsola-Malpighi, 40138, Bologna, Italy

^c Health Sciences and Technologies Interdepartmental Center for Industrial Research (HSTICIR), University of Bologna, 40126, Bologna, Italy

ABSTRACT

Several organ-on-chip and cell-on-chip devices have been reported, however, their main drawback is that they are not interoperable (i.e., they have been fabricated with customized equipment, thus cannot be applied in other facilities, unless having the same setup), and require cell-culture facilities and benchtop instrumentation. As a consequence, results obtained with such devices do not generally comply with the principles of findability, accessibility, interoperability, and reusability (FAIR). To overcome such limitation, leveraging cost-effective 3D printing we developed a bioluminescent tissue on-a-chip device that can be easily implemented in any laboratory. The device enables continuous monitoring of cell co-cultures expressing different bioluminescent reporter proteins and, thanks to the implementation of new highly bioluminescent luciferases having high pH and thermal stability, can be monitored via smartphone camera. Another relevant feature is the possibility to insert the chip into a commercial 24-well plate for use with standard benchtop instrumentation. The suitability of this device for 3D cell-based biosensing for monitoring activation of target molecular pathways, i.e., the inflammatory pathway via nuclear factor kappa-B (NF- κ B) activation, and general cytotoxicity is here reported showing similar analytical performance when compared to conventional 3D cell-based assays performed in 24-well plates.

1. Introduction

In vitro cell-based assays are widely employed to obtain data about biological activity, toxicity and side effects of pure compounds, environmental, and biological samples (D'Alessandro et al., 2016; Schenone et al., 2013). These assays in fact can provide clues on mechanism of action at cellular and subcellular level of environmental contaminants and complex samples. This holistic approach provides complementary information to that obtained with standard analytical techniques (Włodkowiec and Jansen, 2022). Although two-dimensional (2D) cell models are still considered the "gold standard" for cell-based assays, a growing body of evidence suggests that they fail to replicate the *in vivo* complexity and actual cellular architecture comprising the extracellular matrix (ECM) microenvironment (Jensen and Teng, 2020). Instead, 3D cell culture systems overcome many of the limitations of traditional 2D cell culture systems, more closely mimicking the complex phenotypic heterogeneity of living organisms. In fact, 3D cellular systems reproduce cell-cell and cell-matrix interactions, intra- and inter-cellular signalling networks, as well as diffusion/transport processes, which are important for differentiation, proliferation, and various cellular functions (Lan-gans, 2018). At a regulatory level several efforts have been directed by the European Union, the USA, and other nations to replace animal

testing with *in vitro* assays and *in silico* methods. The FDA Modernization Act 2.0 (2022) for the first time amended the Federal Food, Drug, and Cosmetics Act, passed in 1938, eliminating the need for new drugs to undergo animal testing (Han, 2023).

Therefore, current research is currently focused to develop 3D cell models to replace 2D cell cultures and, in the future, also animal models. Different methods and strategies have been explored to obtain 3D cell model, relying on biocompatible supports or rotary cell culture systems (Vakhshiteh et al., 2023; Żuchowska et al., 2024). Standardization of these models is essential to achieve reliable and repeatable outcomes, especially regarding size and shape of 3D models and it still represents one of the bottlenecks for the successful replacement of 2D cell cultures. In addition, there is an unmet need for non-destructive monitoring solutions for 3D cell models (Cortesi and Giordano, 2022). In scientific literature a wide range of different systems have been reported, based either on scaffold-free and scaffold-supported 3D culture systems, however most of them targeted to single applications. Conversely, the pharmaceutical sector is looking for standardized 3D culture methods with effective read-out, ease of automation, and reasonable costs (Fang and Eglén, 2017). These requirements are even more strict for cell-based assays relying on bioluminescence (BL) detection, requiring microscopes equipped with highly sensitive light detectors (e.g., EM-CCD cameras)

* Corresponding author. University of Bologna, Dept. of Chemistry "Giacomo Ciamician", Via P. Gobetti 85, 40129, Bologna, Italy.

E-mail address: elisa.michelini8@unibo.it (E. Michelini).

<https://doi.org/10.1016/j.bios.2024.116454>

Received 23 April 2024; Received in revised form 27 May 2024; Accepted 29 May 2024

Available online 31 May 2024

0956-5663/© 2024 The Authors. Published by Elsevier B.V. This is an open access article under the CC BY license (<http://creativecommons.org/licenses/by/4.0/>).

and light-tight enclosures to protect from ambient light (Araújo-Gomes et al., 2023).

BL, i.e., the spontaneous emission of light observed in several organisms including bacteria, beetles, molluscs, and coelenterates, is generated through a chemical reaction in which an enzyme (luciferase) oxidises a substrate (luciferin), leading to the emission of photons. For some luciferases these reactions require the presence of cofactors such as ATP and Mg^{2+} (Schramm and Weiß, 2024). Thanks to recent advancements in optoelectronics, optical fibres and micro-optics, several attempts were recently aimed at providing affordable miniaturized imaging devices. Smartphone-based microscope platforms showed suitable to image cells, micro- and nanoparticles and pathogens (Heggestad et al., 2022; Moehling et al., 2020; Zeinhom et al., 2018). Many of these approaches relied on cell identification and counting based on brightfield and fluorescence microscopy. Fluorescence, thanks to its high signal intensity, plays a major role as imaging technique, both in conventional laboratory settings and in portable devices. However, differently from BL, fluorescence emission needs for an external excitation light source and suffers of signal background in biological samples (Nath et al., 2023). Thanks to the advancements in chemistry and bioengineering, in the last years new synthetic luciferases and luciferin substrates with improved photon emission and stability have been developed (Calabretta et al., 2023; Yao et al., 2018) and implemented in portable biosensing platforms with smartphones, CCD and CMOS (Belkin and Cheng, 2023; Calabretta et al., 2022a; Cevenini et al., 2016).

We hereby report a smartphone interfaced bioluminescence microfluidic tissue on-a-chip device for multiplexed biosensing, which has been designed to be customized according to specific needs and does not require any special instrumentation. Differently from other microfluidic chip previously reported (Araújo-Gomes et al., 2023), this device is entirely made by 3D printing and used for 3D cell-based biosensing with bioluminescent co-cultures of different cell lines. An extensive analytical characterization of the microfluidic chip device embedding bioluminescent 3D co-cultures was performed even in non-standard cell culture conditions. The possibility to keep the system at room temperature and non-controlled CO_2 conditions is undeniably an asset and a novelty in this field. Generally, all these devices are kept in CO_2 incubators at 37 °C, thus requiring cell culture facilities and equipped laboratories. Instead, we demonstrated that the novel bioluminescent reporter proteins guarantee satisfying analytical performance of the bioassays for inflammation and toxicity.

The microfluidic chip can house co-cultures and microtissues and can be attached, via a 3D printed compact optical set-up to a portable microscope and the rear camera of a smartphone. We developed and optimized a simple assay procedure to obtain spheroids also at room temperature and non-controlled CO_2 conditions. The 3D microfluidic printed device is a cost-effective and sustainable tool for rapid analysis of 3D co-cultures and microtissues without the need of laboratory-grade microscopes, low-light detectors, or sophisticated optical set-ups. We demonstrated the feasibility of the approach by performing a dual assay for general cytotoxicity and inflammatory activity, the latter via NF-KB pathway monitoring. The good analytical performance of this approach demonstrates the possibility to enlarge the accessibility of bioluminescence imaging assays to researchers without specialized cell imaging facilities.

2. Materials and methods

2.1. Chemicals and reagents

Human embryonic kidney (HEK293T) cells, Human Dermal Fibroblast (HDF) cells and HeLa cells from cervical carcinoma were from ATCC (American Type Culture Collection [ATCC], Manassas, VA, USA). Cell culture reagents and materials were from Carlo Erba Reagents (Cornaredo, Milano, Italy), the enzymes required for cloning procedures were from Fermentas (Vilnius, Lithuania). Plasmid extraction kits,

beetle luciferin potassium salt (D-luciferin) and BrightGlo substrate were from Promega (Madison, WI, USA). Tumor Necrosis Factor- α (TNF α , purity higher than 95%), dimethyl sulfoxide (DMSO), Micro-Tissues® 3D Petri Dish® micromold spheroids size L 7 × 14 array, and all other chemicals were purchased from Sigma-Aldrich (St. Louis, MO, USA). The mammalian expression plasmids pGL4.32_Nf κ B_Luc2P and pGL4.74[hRluc/TK] carrying Luc2P luciferase under the regulation of NF- κ B transcriptional regulation and hRluc under Herpes simplex virus thymidine kinase promoter (TK) were from Promega. Plasmids BgLuc, BoLuc and BrLuc luciferase genes were obtained as previously described (Calabretta et al., 2023). The reporter vectors pCMV_BgLuc, pCMV_BoLuc, pCMV_BrLuc, pTK_BgLuc, and pNF κ B_BrLuc were obtained by standard molecular cloning procedures.

Bioluminescent measurements were performed with Varioskan LUX multimode microplate reader (ThermoFisher Scientific). Oneplus6 smartphone (Oneplus, Shenzhen, China) equipped with an integrated camera (1/2.8" 16 MP Sony IMX 398 sensor, 1.12 μ m pixel size and F1.7 aperture) was used as portable light detector. 60x LED UV portable mini-microscope was from Tenyua (China). 3D printer and clear biocompatible resin were from Formlabs.

2.2. *In vivo* imaging simulation of luciferase mutants

Purified BgLuc luciferase (from 0.6 to 0.07 mg/mL), BoLuc luciferase (from 0.6 to 0.07 mg/mL) and BrLuc luciferase (from 0.6 to 0.07 mg/mL) were obtained as previously described (Calabretta et al., 2023) and used for *in vivo* imaging simulation studies using chicken meat breast cut at different thickness (from 0.0 to 2.5 mm). 10 μ L-aliquots of purified luciferases were dispensed in a white 394 well plate, then 10 μ L of Bright-Glo substrate was added and wells covered with meat slices of different thickness (1.5, 2.0 and 2.5 mm). BL measurements were performed in duplicate, and experiments repeated at least three times. For the detection OnePlus6 smartphone was used with an integration time of 30 s and ISO 3200.

2.3. Expression and characterization of BgLuc, BoLuc and BrLuc luciferase mutants in HEK293T 3D cell models

HEK293T cells were grown routinely in 5% CO_2 in air in minimum essential medium with Earle's salts (DMEM) supplemented with 10% (v/v) fetal bovine serum, 2 mM L-glutamine, 0.1 mM non-essential amino acids, MEM vitamins, and antibiotic/antimycotic solution.

Cells, previously seeded in a flat-bottom clear 24-well plate at a density of 8.0×10^4 cells/well, were transiently transfected with pcDNA3.1-BgLuc, pcDNA3.1-BoLuc or pcDNA3.1-BrLuc expression vectors using the FUGENE® HD transfection reagent at a ratio of 1:3 and incubated under standard conditions for 24 h at 37 °C and 5% CO_2 . To obtain 3D spheroids, 100 μ L of complete culture medium was added to each well of a Corning® Elplasia® 96-well microspace round-bottom cell culture plates, followed by 200 μ L of cell suspension containing 3.0×10^4 cells per well, and let to incubate at 37 °C and 5% CO_2 for spheroid formation. Emission kinetics (20 min with 200 ms integration time) were obtained in 2D cell format and 3D models with the luminometer Thermo Scientific Varioskan LUX Multimode Microplate Reader after injection of 60 μ L of D-Luciferin (D-LH₂) citrate solution 1.0 mM pH 5.0 or with 50 μ L of the lysing BrightGlo substrate while emission spectra were recorded from 450 to 750 nm, at 2-nm intervals with 1000-ms integration time. Smartphone based detection of luciferase mutants expressed in 3D mammalian cells was performed using HEK293T 72 hour-old spheroids. Spheroids were treated with trypsin 1x, then cells were counted and transferred at 1.0×10^4 cells/well concentration in a black 384-well small volume plate. Serial dilutions from 30 to 5.0×10^3 cells/well of the green, orange and red-emitting HEK293T were prepared, seeded in the same plate and imaged after addition of 5 μ L BrightGlo substrate with the smartphone camera by integrating BL signals for 30 s with ISO 3200. All measurements were performed in

triplicate and repeated at least three times. The limit of detection (LOD) was calculated as the number of cells expressing BgLuc, BoLuc or BrLuc luciferases providing a BL signal corresponding to the blank signal plus three times its standard deviation. Blank signal was obtained by measuring same number of non-transfected cells.

2.4. Design and fabrication of microfluidic chip

The microfluidic chip device was designed using a CAD software (SketchUp, Trimble Inc.) and 3D-printed in clear photopolymerizable and autoclavable resins employing a Form 2 stereolithography (SLA) 3D printer (Formlabs Inc.). 3D printing was performed using a 50- μm layer thickness (the horizontal resolution of the 3D printer is about 100 μm) to obtain adequate printing of small details (e.g., fluidic inlets). The device consists of three components: a) a holder for the gel support for 3D growing of cells, b) a container for cell culture medium, c) a cover including fluidic in and outlet ports (Figure 3B, C, D).

The container cover comprises fluidic inlet and outlet which are connected to microperistaltic pumps (RP-Q2 miniature peristaltic pump, Takasago Electric, Inc., Nagoya, Japan). The pumps have been modified by installing a 3D-printed pump head to accommodate a smaller silicone tubing (0.5 mm I.D., 1.0 mm O.D.) in order to reduce nominal flow rate to 100 $\mu\text{L}/\text{min}$. When activated, the pumps replace the medium in the container or provide the sample to be analyzed.

2.5. Multiplexed inflammation/toxicity assay

The dual-reporter assay was optimized using the BgLuc and BrLuc luciferases expressed in HeLa cells. HeLa cells were previously co-transfected in a 24 clear well-plate with 0.1 μg of the plasmid pTK_BgLuc encoding for the green-emitting luciferase as viability control and with 0.4 μg of the red emitting luciferase under the control of NF- κB response elements pNF κB _BrLuc. After 24 h post-transfection a co-culture of HeLa (2.0×10^4 cells) and HDF cells (0.5×10^4 cells) was prepared in 75 μL of DMEM and then seeded in the 3D Petri Dish® previously equilibrated and accommodated into the printed holder. The holder was placed in the container, closed with the cover and the medium delivered through the inlet port at a flow rate of 100 $\mu\text{L}/\text{min}$. The time taken to fill the entire chip with the medium allows the cells to settle in the microcavities of the agarose support by gravity. The microfluidic chip was then placed in the incubator at 37 °C for spheroid formation. After 48 h, the microfluidic chip containing spheroids was treated with TNF α solution delivered in the microfluidic chip for 5 h. TNF α dilutions, concentration range from 0.1 to 20 ng/mL, were used to treat in duplicate 3D spherical microtissues directly in the microfluidic chip. Culture medium was used as a control (blank). After treatment the holders were transferred in a 24 clear well-plate for performing BL analysis (emissions kinetics acquired for 20 min with 500 ms integration time) by adding the BrightGlo substrate with the Varioskan™ LUX multimode microplate reader using F545 (510–580 nm) and F615 (590–640 nm) high transmittance band-pass emission filters BL intensities were calculated as ratio between the contribution of the red and green emitting signals. The mean value of each corrected BL signal was plotted as fold response over the TNF- α control. The half maximal effective concentration (EC50), which is the concentration of the TNF α producing 50% of the maximum response, was calculated using the equation: $Y = \text{Bottom} + (\text{Top} - \text{Bottom}) / (1 + 10^{-(\text{LogEC50} - X) \times \text{Hillslope}})$, where X is the logarithmic concentration of TNF α .

2.6. Smartphone-based toxicity assay

Toxicity assay was performed using the microfluidic chip platform based on smartphone coupled with a portable low-cost microscope. HEK293T cells were previously genetically engineered with reporter plasmid pCMV_BoLuc in a clear bottom 24 well-plate at a density of 8×10^4 cells per well, with 500 μL of complete growth medium. Briefly 24 h

post transfection, co-cultures of HDF and HEK293T with 0.5×10^4 and 2.0×10^4 cells, respectively were obtained in 75 μL volume of medium and seeded in the MicroTissues® 3D Petri Dish® accommodated in the microfluidic chip holder to obtain spheroids with a diameter approximately of 180 μm . The holder was placed into the container, close with the cover and the medium delivered through the inlet port at a flow rate of 100 $\mu\text{L}/\text{min}$. The microfluidic chip was then placed in the incubator at 37 °C for spheroid formation. After overnight incubation, the microfluidic chip containing spheroids was treated with DMSO solution delivered continuously in the microfluidic chip for 90 min. DMSO solution from 0.1 to 20 % (v/v) were prepared in medium and used to treat in duplicate 3D spherical microtissues in the microfluidic chip while culture medium was used as a control (blank). After DMSO treatment, to perform BL analysis the medium was removed by the outlet port and a volume of 50 μL of D-LH₂ was added in the holder containing cells. OnePlus 6 interfaced with a low-cost portable microscope was used to acquire BL signal (30 s, ISO 3200). ImageJ software (National Institutes of Health, Bethesda, MD) was used to analyse images while GraphPad Prism v.8.0 (GraphPad Software, La Jolla, USA) to plot the data. The IC₅₀, half maximal inhibitory concentration, which is the concentration of the inhibitor needed to inhibit a biological process or response by 50%, was calculated using the following equation:

$$Y = \text{Bottom} + (\text{Top} - \text{Bottom}) / (1 + 10^{-(X - \text{LogIC50}) \times \text{Hillslope}})$$

where X is the logarithmic concentration of DMSO, and Y is the BL response. All measurements were performed in triplicate and repeated at least three times in different days.

3. Result and discussions

Several methods are available to obtain 3D cell cultures (Jensen and Teng, 2020; Żuchowska et al., 2024), however, the standardization of 3D cell models is the main bottleneck which, together with difficulty of manipulation and high handling costs, severely affect the possibility to obtain robust and reproducible results within contained cost and reduced carbon footprint. The integration of 3D cell models with microfluidics partially overcome some of these limitations, also reducing reagents volumes and increasing reproducibility of the results. Microfluidic devices for drug testing in static and dynamic 3D cell cultures have been reported using glass and polymers such as polymethylmethacrylate (PMMA) or polydimethylsiloxane (PDMS), yet requiring the fabrication of multi material devices and customized set up (Araújo-Gomes et al., 2023; Do et al., 2023).

Moreover, the possibility to integrate cells engineered with multiple reporter genes which enable easy monitoring of physiological processes by luminescence measurements (e.g., bio-chemiluminescence and fluorescence) in such microfluidic devices would greatly expand the relevance and quality of information gathered with the device.

However, none of these systems fully addressed all the requirements of i) flexibility, thanks to possibility of repurposing the device via 3D printing ii) suitability for integration with portable detectors for point-of-care and point-of-need analysis, i.e., to enable analysis of inflammation of clinical samples using a smartphone, iii) compatibility with commercial benchtop instrumentation, iv) low-cost and low carbon footprint. As a consequence, results obtained with such devices do not generally comply with the principles of findability, accessibility, interoperability, and reusability (FAIR).

We here addressed these issues and designed a microfluidic device for real time detection of BL to monitor molecular pathways, target bioactivities, or detect analytes of clinical and environmental interest. The chip enables multiplexed analysis in 3D microtissues of cells engineered to express BL reporter proteins emitting at different wavelength and requiring the same substrate.

To provide enhanced sensitivity we employed newly developed luciferase mutants with improved BL emission and stability, i.e., BgLuc,

BoLuc and BrLuc. BgLuc is a green-emitting luciferase characterized by a λ_{\max} of 548 nm (Fig. S1A) and a half bandwidth of 72 nm (Calabretta et al., 2022b). BoLuc is an orange-emitting luciferases with a λ_{\max} of 600 nm and half bandwidth of 72 nm (Fig. S1B), while the BrLuc is a red-emitting luciferase characterized by λ_{\max} of 615 nm and half bandwidth of 60 nm (Fig. S1A) (Calabretta et al., 2023).

A biosensing platform was developed in which spheroids composed by co-cultures of genetically engineered cells are directly grown inside a 3D printed microfluidic chip. The 3D printed chip comprises an holder for the agarose-supported self-assembled 3D microtissue, an external container for liquid medium and a cover.

3.1. Luciferase mutants BL characterization and *in vivo* imaging simulation

To assess the performance of these luciferases as reporter proteins in 3D spherical microtissues in terms of photon light emission, *in vivo* imaging simulations were performed in 384-well microtiter plates using aliquots of different concentrations of purified BgLuc, BoLuc and BrLuc enzymes (concentration range from 0.07 to 0.6 mg/mL) covered with slices of chicken meat (thickness from 0.0 to 2.5 mm) (Fig. 1A). The introduction of the mutation S284T in the human codon optimized version of BgLuc luciferase, allowed to obtain a very bright emitting orange luciferase, together with other three mutations V241I/G246A/F250S which account for increased intensity and a modest blue-shift which is counteracted by the S284T mutation previously introduced into the BgLuc luciferase (Calabretta et al., 2023). After addition of the Bright-Glo substrate, signals were acquired with OnePlus6 smartphone camera for 30 s and ISO 3200 (Fig. 1B). As concerns the emission intensities of the purified luciferase mutants, BoLuc showed BL intensities of about two and three times higher than BgLuc and BrLuc luciferase, respectively (Fig. S2). As shown in Fig. 1C, BL intensities from BgLuc luciferase decreased with the increase of thickness of the chicken meat, with a BL decrease of about 54, 66 and 80% for 1.5, 2.0 and 2.5 mm thickness, respectively. On the contrary, for the BoLuc luciferase we observed similarly decreased BL intensities of about 39 and 35% for 1.5

and 2.0 mm, respectively and of about 70% for 2.5 mm thickness. A similar behaviour was observed for the red-emitting BrLuc luciferase, with a BL decrease of about of 35, 30 and 65% for 1.5, 2.0 and 2.5 mm thickness, respectively. These results confirmed that photons at wavelength longer than 600 nm are able to penetrate more easily through tissues, making BoLuc and BrLuc suitable candidates for *in vivo* imaging. However, if the total light emission is considered, the broader emission peak, together with higher intensity of BoLuc, accounts for improved detectability. In fact, if we consider the images taken with the 2.5 mm thick slice covering BoLuc and BgLuc aliquots, total light emissions were 50.3 ± 0.6 and 17.5 ± 1.8 RLU, respectively. The same behaviours were observed by decreasing the concentration of purified luciferase enzymes (0.3, 0.15 and 0.07 mg/mL) (Fig. S3).

3.2. Bioluminescence characterization of green-, orange- and red-emitting 3D spheroids with the smartphone

To understand the detection of BL emission in living cells exploiting complementary metal-oxide semiconductor (CMOS) smartphone camera, we preliminary evaluated the minimum number of detectable HEK293T cells expressing BgLuc, BoLuc and BrLuc luciferase mutants. To this end, a 10 μ L-volume of cell dilutions (from 30 to 1.0×10^4 cells) was dispensed in a black 384 microwell plate and imaged with the OnePlus 6 smartphone camera after addition of 5 μ L of BrightGlo substrate (Fig. 2A). The limits of detection, calculated as the cell number leading to a BL signal corresponding to that of the blank plus three standard deviations, were about 30, 40 and 70 cells for the BgLuc, BoLuc and BrLuc luciferases, respectively, demonstrating the suitability of these luciferase mutants as reporter proteins in 3D cell models (Fig. 2B). It must be pointed out that these results were obtained with a lysing substrate, thus providing the detectability of luciferase mutants irrespectively of their light signal obtained within the cells.

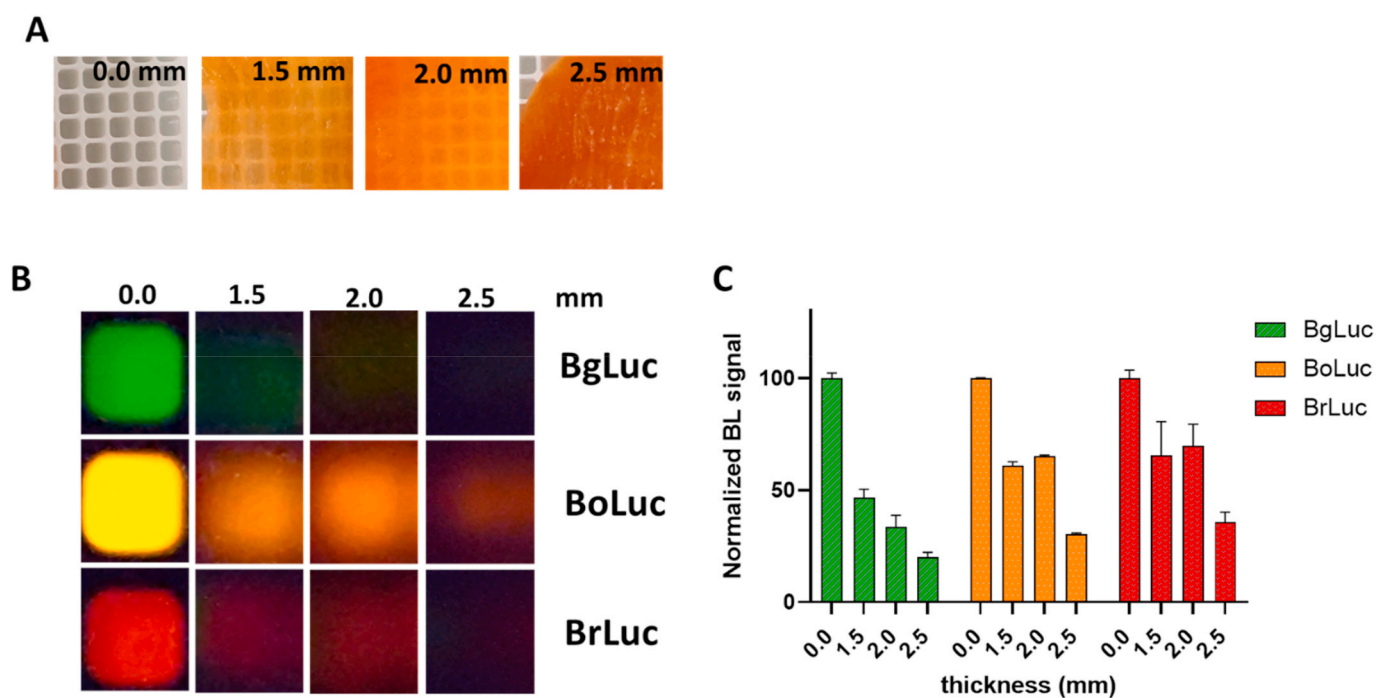


Fig. 1. *In vivo* imaging simulation of purified BgLuc, BoLuc and BrLuc luciferases: A) image of the white 384 well-plate covered with chicken meat slices of different thickness (0.0, 1.5, 2.0 and 2.5 mm); B) Images of the purified BgLuc, BoLuc and BrLuc luciferases obtained with OnePlus6 (30sec ISO 3200) after the addition of the BrightGLO substrate and corresponding BL signals (C).

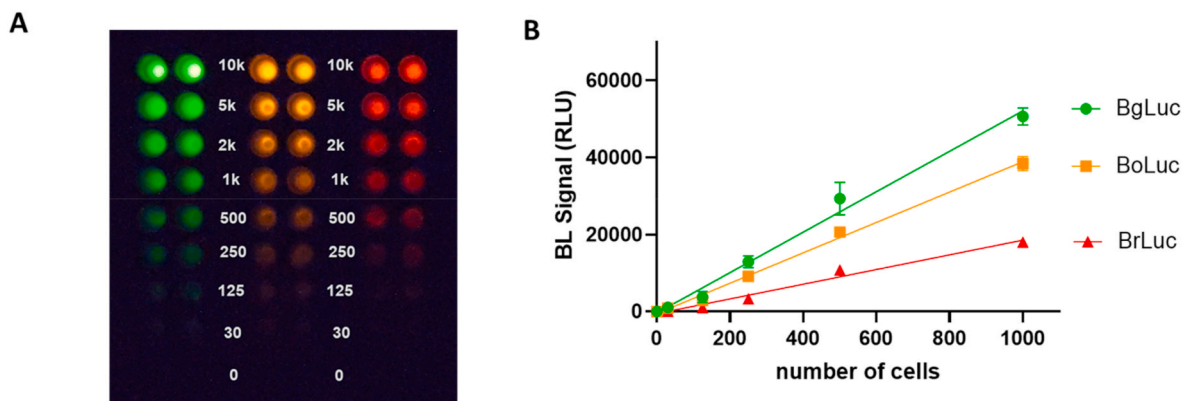


Fig. 2. Characterization of BgLuc, BoLuc and BrLuc luciferase mutants in 3D Human embryonic kidney cells. A) BL image of serial dilution of cells transfected with BgLuc, BoLuc and BrLuc luciferases, seeded in duplicate in a black 384 small volume wellplate, obtained with the OnePlus 6 smartphone (integration time 30 s, ISO 3200) after addition of the commercial BrightGlo substrate; B) Elaboration of BL image with ImageJ software to quantify the BL signal of each well and to calculate the minimum number of detectable cells expressing the BgLuc, BoLuc and BrLuc luciferases.

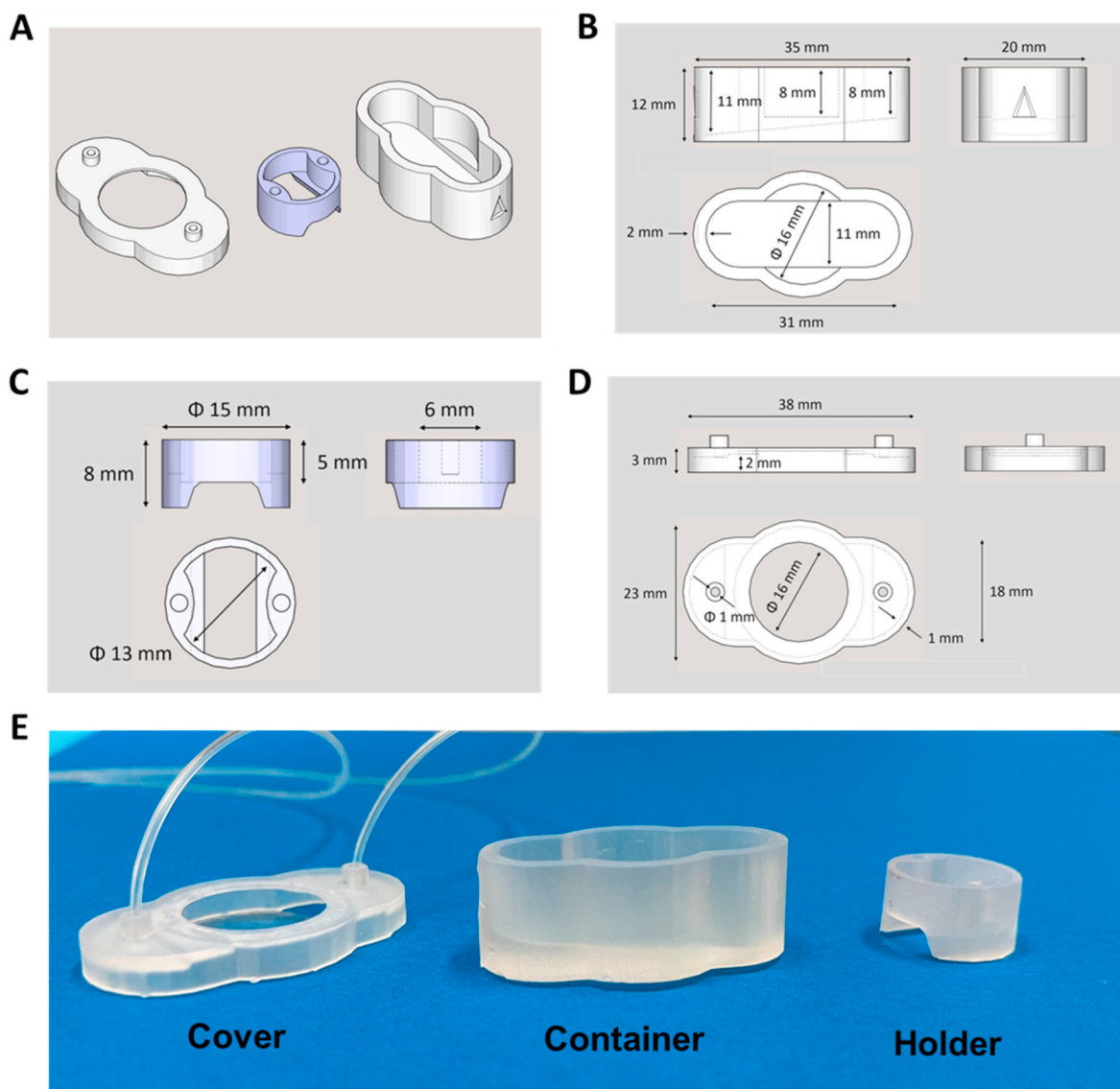


Fig. 3. Microfluidic chip: A) overview of the three components of the device designed with SketchUp Software B) design of the container, C) the holder, and D) the cover; E) 3D printed microfluidic chip components obtained with Formlabs 3D printer.

3.3. Microfluidic chip embedding BL 3D microtissues: design and characterization

The microfluidic chip includes a holder, a container, and a cover with fluidic connections (Fig. 3A–D). The holder (15 mm diameter and 8 mm height) allows easy manipulation of the gel support (e.g., for transferring the gel in a conventional 24-well microplate) and is designed according to the shape of the gel (Fig. 3C). Furthermore, its diameter fits the wells of a conventional 24-well microtiter plate, representing an advantage for BL multiplexing analysis also with low light intensities, by using benchtop luminometers equipped with band pass filters. Once the holder with the gel is inserted in the container, the lower part of the gel is in contact with the culture medium to allow free diffusion of nutrients from the medium to the gel and then to the microwells containing the 3D cultured cells.

The inner volume of the container is about 2.5 mL and its shape allows easy removal of the culture medium (e.g., for replacing the medium or adding a new medium supplemented with target analytes) (Fig. 3B). In the proposed version of the device, a transparent window (e.g., made of a transparent polymer such as polyacrylate) or glass allows visual inspection and imaging of the gel without removing the cover. The fluidic connections are equipped with flexible silicone rubber tubes (1.0 mm O.D.) for continuous replacement of the culture medium (Video S1).

The microfluidic platform integrates agarose gel supports containing self-assembled 3D microtissues. The non-adhesive agarose gel support contains cylindrical microwells created using a reusable 5 × 7 array micro-mold with 800 μm diameter rounded pegs.

3.4. Optimization of 3D cell co-cultures

To obtain robust and reproducible results a key factor is the standardization of 3D cell models in terms of size and shape. To this end, monitoring of microtissue formation was performed by using Thermo Scientific Invitrogen Evos M5000 Imaging Systems using a 4X objective. Uniform size of HEK293T and HDF co-culture was obtained after two days, with an average spheroid diameter of 150 ± 22, 115 ± 25 and 105 ± 30 μm for the proportions of co-cultures 4:1, 3:2 and 2:3, respectively (Fig. S4).

Concerning results obtained with co-cultures of HeLa and HDF cells, average spheroid diameters of 165 ± 25, 140 ± 15 and 90 ± 15 μm were obtained using cell proportions of 4:1, 3:2 and 2:3, respectively (Fig. S5). This difference is probably due to a different surface tension of fibroblast aggregates which may cause a reduction in the size of the spheroids (Kosheleva et al., 2020). According to literature (Lambrechts et al., 2014), in all these spheroids, having a diameter of less than 200 μm, less than 2% of the cells should be comprised in the internal hypoxic core, thus not altering BL measurements that require molecular oxygen.

3.5. Multiplexed inflammation/toxicity biosensor

A dual biosensor was developed for monitoring inflammatory activity and toxicity in the same sample. We used co-cultures of HeLa and HDF cells in which only HeLa were engineered either with TK_BgLuc, a plasmid for constitutive expression of BgLuc, or NFκB-BrLuc, a plasmid with BrLuc under the regulation of NFκB transcription factor, a key mediator of inflammatory responses. The activation of intracellular inflammatory pathways leads to the expression of BrLuc. Therefore, the BL intensity deriving from BrLuc is proportional to the inflammatory response of the cell. To correct the analytical signal according to cell viability and increase the robustness of the biosensor, an internal viability control, i.e., the Bgluc luciferase, was introduced. These luciferases require the same substrate, D-luciferin and provide well separated emission spectra thus simplifying the detection steps, reducing the cost and improving the sustainability, in accordance with the principles of green and white analytical chemistry (Nowak et al., 2021). We selected to target the transcription factor NF-κB because is one of the

signal-activated transcription factor aberrantly activated in many carcinomas (Escárcega et al., 2007). In this case we exploited the flexibility of the device, which includes an *ad hoc* designed holder that fits the wells of a commercial 24-well microplate. Therefore, multiplexed analysis was first performed with a benchtop luminometer using optical band-pass filters to acquire the BL signals from the green and the red-emitting luciferases (Fig. 4A). After 5 h of incubation time a TNF-α dose-response curve was obtained showing a LOD of 0.14 ± 0.05 ng/mL and an EC₅₀ of 0.9 ± 0.4 ng/mL (Fig. 4B). These results are in line with previously reported assays based on 3D spheroids obtained with commercial micro-patterned plates but with the advantage of analysing both inflammatory activity and toxicity (Calabretta et al., 2023).

3.6. Smartphone-based 3D cell toxicity biosensor

A BL toxicity biosensor was obtained using a co-culture of HDF cells and BL HEK293T cells genetically engineered with the BoLuc luciferase under the control of a constitutive promoter (CMV). Since BL intensity correlates to the metabolic state of the cell it can be used as a real-time measure of cell viability. HEK293T cells were selected because they showed suitable for assessing the toxicity and bioactivity of drugs and environmental samples (Li et al., 2015). Besides, thanks to their high transfection efficiency and rapid capability to form 3D cell aggregates, they are a good candidate for biosensor integration and implementation of 3D cell models. The orange emitting luciferase mutant (BoLuc) was selected as reporter protein thanks to its broad BL emission spectrum (λ_{max} : 600 nm, half bandwidth: 72 nm) provided the maximum light output in simulated *in vivo* imaging experiments performed with the smartphone CMOS. In perspective of having a ready-to-use device for biosensing applications, 3D co-cultures were obtained directly in the microfluidic chip. Co-culture spheroids with a diameter of 150 ± 30 μm were obtained by seeding 2.0 × 10⁴ HEK293T cells and 0.5 × 10⁴ HDF cells in 75 μl of medium in 3D Petri Dish®. These numbers of cells were selected in order to obtain an average spheroid size less than 200 μm according to the 3D Petri Dish® Manufacturer instructions and the 4:1 proportion of HEK293T/HDF cells allowed to obtain a diameter of about 150 μm with a proportion which mimics the *in vivo* tumor microenvironment. Two days after transfection BL detection was performed both with a benchtop luminometer and with a smartphone connected to a pocket microscope having a cost of 5 euro via a 3D printer adaptor. To prompt use without further cell facilities the implementation of L15 medium was also evaluated. This medium is specifically formulated to enable cell growth without CO₂ equilibration (Delmotte et al., 2002). The results shown in Fig. S6 were obtained by using HEK293T transfected with pCDNA_BgLuc incubated for 5 days at room temperature (25 °C and uncontrolled atmosphere conditions, i.e., no use of CO₂ incubator for cell cultures). As shown in Fig. S6 L15 medium enabled efficient growth of cells even at room temperature (23 °C). Since cells were kept in the bench of the laboratory, antibiotic supplementation (100 U/μL penicillin, and 100 μg/mL streptomycin) was used to avoid contamination with bacteria or mold. In all the experiments no contamination was reported, thus supporting the feasibility of this approach.

Dose-response curves for DMSO were obtained with HEK293T spheroids at 30, 60 and 90 min (37 °C, 5% CO₂) obtaining LODs of 1.8, 1.1 and 0.4 % v/v, respectively (Fig. 4C). As concerns the analytical performance, LODs for DMSO (0.4 % v/v) with cells grown in L15 medium at 37 °C or at 23 °C of 2.3 % v/v were obtained, with an IC₅₀ of 1.1 and 5.3 % v/v, respectively (Fig. 4D) demonstrating the suitability of using the cell microfluidic chip even in suboptimal conditions or for use in laboratories not equipped with cell culture facilities. Fig. 4E shows HEK293T spheroids transfected with pCDNA-BoLuc imaged with the pocket microscope connected to the smartphone.

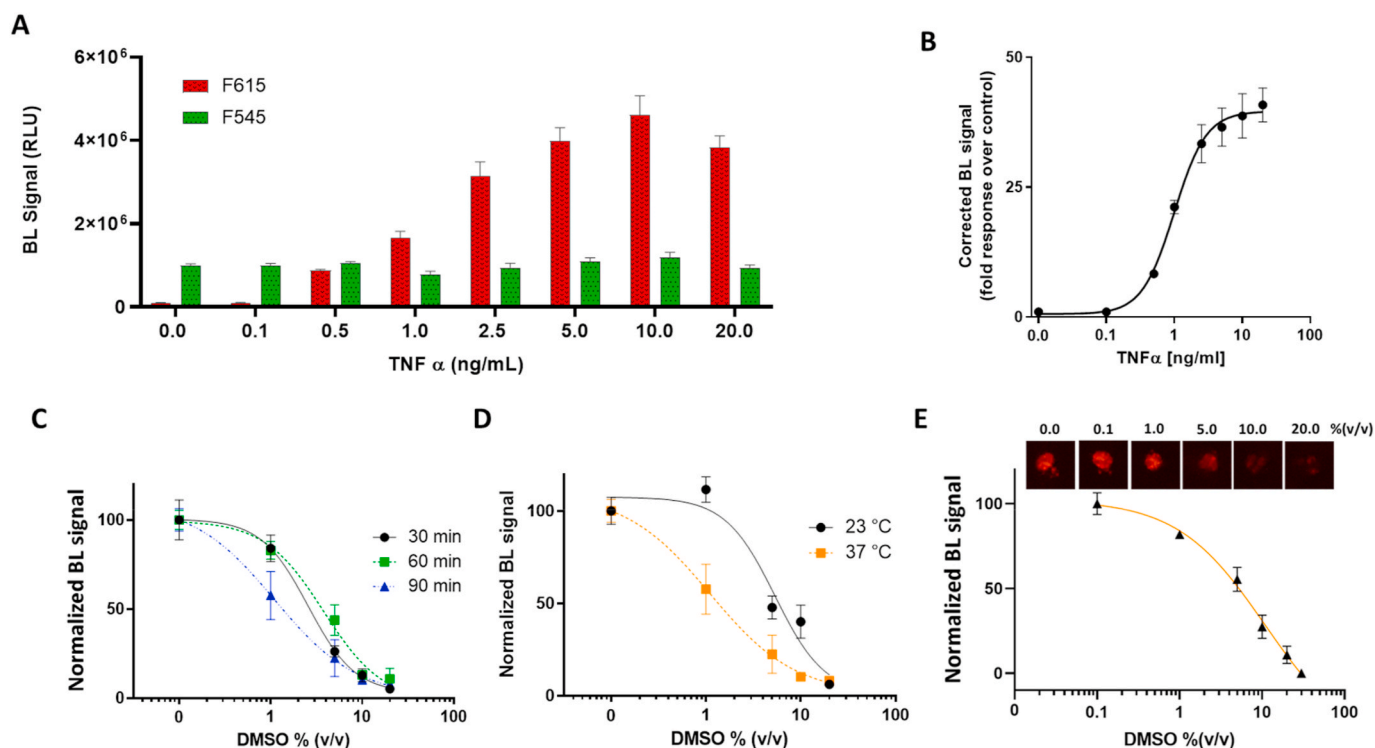


Fig. 4. A) BL intensities measured with benchtop luminometer equipped with optical bandpass filters from HeLA cells genetically engineered with the TK_BgLuc and NF- κ B_BrLuc and grown as 3D co-culture with HFD cells in the microfluidic chip (37 °C, 5% CO₂). B) Corrected TNF α dose-response curve; C) DMSO toxicity curves obtained at 30, 60 and 90 min incubation with HEK293T spheroids genetically engineered with the CMV_BoLuc and grown in L15 medium at 37 °C, 5% CO₂ and D) at 23 °C and without CO₂ controlled atmosphere. E) DMSO toxicity curve obtained in a 3D co-culture of HEK293T genetically engineered with the CMV_BoLuc with HFD cells grown in the microfluidic chip, in the upper panel images of 3D co-cultures taken with a smartphone (30s, ISO 3200) coupled with a 60x LED UV portable mini-microscope are shown.

3.7. Assessment of sustainability of 3D cell-based microfluidic device

The degree of sustainability of the 3D cell-based method relying on the microfluidic device was assessed according to the RGB 12 algorithm (Nowak et al., 2021) which incorporates 12 white analytical chemistry (WAC) principles, allowing to define the whiteness of the method in a transparent and objective way. This approach has been successfully applied to assess the sustainability of other biosensors (Gullo et al., 2024). The algorithm includes red, which denotes analytical efficiency, green, which refers to adherence to green analytical chemistry (GAC) principles, and blue, which denotes practical/economic efficiency and productivity. After evaluation, a color derived from the proportion of each primary color is assigned to the method. A white method, which has a high saturation of each main color, is thus an optimal, comprehensive, and consistent analytical procedure. The darker the method results, and further from white in the RGB color space, the lower is its degree of sustainability. The developed biosensing assays were compared to a previously reported laboratory-based method relying on 3D cells grown in micropatterned plates commercial microplates and benchtop instrumentation and with a previously reported microfluidic device obtained with soft lithography technique in which single cells are maintained into a hydrogel matrix (Araújo-Gomes et al., 2023). Data shown in Supplementary materials report the green and blue scores of these methods as well as the score assessment criteria. As concerns sustainability (green score), the smartphone-based toxicity method ranked first with a remarkable 88.4% score, versus 52.1% of the analogous assay performed with standard methods. Also considering the practicability, the blue score was very high (86.3%), as expected by a method which does not require benchtop or sophisticated instrumentation (e.g., EM-CCD cameras, luminometers and CO₂ incubator).

4. Conclusions

The article reports for the first time the development of a tissue-on-chip device enabling self-assembly of 3D cell models, including co-cultures of two cell-lines, engineered with multiple reporter genes, together with the implementation of bioluminescence detection. Two biosensing applications were developed as proof-of-principle demonstration of the microfluidic chip: a multicolor inflammation/toxicity dual assay and a toxicity smartphone-based screening assay, the latter exploiting a low-cost pocket-size microscope and does not require cell facilities (CO₂ incubators). The analytical performance of these novel biosensing tools was assessed also with not optimized condition (25 °C and uncontrolled atmosphere conditions), demonstrating high potential for future implementation in different fields, including drug screening on patient-derived cancer cells for personalized medicine. To achieve adequate analytical performance we selected, and characterized two novel luciferases, BoLuc and BrLuc, which could be highly valuable in highly demanding applications, such as multicolor reporter gene *in vitro* and *in vivo* biosensing. Differently from previously reported microfluidic chips integrating cell cultures, the reported tissue-on-chip device not only enables easy monitoring of physiological processes by non-invasive bioluminescence imaging but also is characterized by high flexibility, since it is 3D-printed and can easily repurposed, high suitability for integration with portable detectors for point-of-care and point-of-need analysis, compatibility with commercial benchtop instrumentation, as well as low-cost and low carbon footprint. To the best of our knowledge this is the first microfluidic device for 3D cell-based biosensing which has been assessed according to degree of sustainability. To the best of our knowledge this is the first time that an in-depth assessment of sustainability of a 3D cell-based microfluidic device is reported. This evaluation is pivotal for future investigations and development of new

analytical methods relying on devices and we envisage that it will be mandatory for all methods and devices.

Moreover, this novel approach fulfils the requirements necessary to produce FAIR data with great potential for turning cell-based assays into portable 3D cell biosensors.

CRedit authorship contribution statement

Maria Maddalena Calabretta: Writing – review & editing, Writing – original draft, Visualization, Validation, Methodology, Investigation, Formal analysis, Data curation, Conceptualization. **Denise Gregucci:** Investigation, Data curation. **Massimo Guardigli:** Writing – review & editing, Visualization, Methodology, Conceptualization. **Elisa Michelini:** Writing – review & editing, Writing – original draft, Validation, Supervision, Resources, Project administration, Methodology, Investigation, Funding acquisition, Conceptualization.

Declaration of competing interest

The authors declare that they have no known competing financial interests or personal relationships that could have appeared to influence the work reported in this paper.

Data availability

Data will be made available on request.

Acknowledgements

This study was, in part, carried out within the Agritech National Research Center and received funding from the European Union Next-Generation EU National Recovery and Resilience Plan (NRRP), Mission 04 Component 2, investment 1.4—D.D. 1032 June 17, 2022, CN00000022 and investment 1.5—NextGenerationEU, call for tender no. 3277, dated 30/12/2021 and award number: 0001052, dated 23/06/2022. Part of the work was also funded by the European Union's Horizon Europe project FARMWISE under GA No. 101135533.

Appendix A. Supplementary data

Supplementary data to this article can be found online at <https://doi.org/10.1016/j.bios.2024.116454>.

References

- Araújo-Gomes, N., Zambito, G., Johnbosco, C., Calejo, I., Leijten, J., Löwik, C., Karperien, M., Mezzanotte, L., Teixeira, L.M., 2023. Bioluminescence imaging on-chip platforms for non-invasive high-content bioimaging. *Biosens. Bioelectron.* 237, 115510 <https://doi.org/10.1016/j.bios.2023.115510>.
- Belkin, S., Cheng, J.-Y., 2023. Miniaturized bioluminescent whole-cell sensor systems. *Curr. Opin. Biotechnol.* 82, 102952 <https://doi.org/10.1016/j.copbio.2023.102952>.
- Calabretta, M., Gregucci, D., Martínez-Pérez-Cejuela, H., Michelini, E., 2022b. A luciferase mutant with improved Brightness and stability for whole-cell bioluminescent biosensors and in vitro biosensing. *Biosensors* 12 (9), 742. <https://doi.org/10.3390/bios12090742>.
- Calabretta, M.M., Gregucci, D., Michelini, E., 2023. New synthetic red- and orange-emitting luciferases to upgrade *in vitro* and 3D cell biosensing. *The Analyst* 148 (22), 5642–5649. <https://doi.org/10.1039/D3AN01251D>.
- Calabretta, M.M., Lopreside, A., Montali, L., Zangheri, M., Evangelisti, L., D'Elia, M., Michelini, E., 2022a. Portable light detectors for bioluminescence biosensing applications: a comprehensive review from the analytical chemist's perspective. *Anal. Chim. Acta* 1200, 339583. <https://doi.org/10.1016/j.ajca.2022.339583>.
- Cevenini, L., Calabretta, M.M., Lopreside, A., Tarantino, G., Tassoni, A., Ferri, M., Roda, A., Michelini, E., 2016. Exploiting NanoLuc luciferase for smartphone-based bioluminescence cell biosensor for (anti)-inflammatory activity and toxicity. *Anal. Bioanal. Chem.* 408 (30), 8859–8868. <https://doi.org/10.1007/s00216-016-0062-3>.
- Cortesi, M., Giordano, E., 2022. Non-destructive monitoring of 3D cell cultures: new technologies and applications. *PeerJ* 10, e13338. <https://doi.org/10.7717/peerj.13338>.
- D'Alessandro, S., Camarda, G., Corbett, Y., Siciliano, G., Parapini, S., Cevenini, L., Michelini, E., Roda, A., Leroy, D., Taramelli, D., Alano, P., 2016. A chemical susceptibility profile of the *Plasmodium falciparum* transmission stages by complementary cell-based gametocyte assays. *J. Antimicrob. Chemother.* 71 (5), 1148–1158. <https://doi.org/10.1093/jac/dkv493>.
- Delmotte, P., Degroote, S., Lafitte, J.-J., Lamblin, G., Perini, J.-M., Roussel, P., 2002. Tumor Necrosis factor α increases the expression of Glycosyltransferases and Sulfotransferases responsible for the Biosynthesis of sialylated and/or sulfated lewis x epitopes in the human bronchial mucosa. *J. Biol. Chem.* 277 (1), 424–431. <https://doi.org/10.1074/jbc.M109958200>.
- Do, T.D., Pham, U.T., Nguyen, L.P., Nguyen, T.M., Bui, C.N., Oliver, S., Pham, P., Tran, T. Q., Hoang, B.T., Pham, M.T.H., Pham, D.T.N., Nguyen, D.T., 2023. Fabrication of a low-cost microfluidic device for high-throughput drug testing on static and dynamic cancer spheroid culture models. *Diagnostics* 13 (8), 1394. <https://doi.org/10.3390/diagnostics13081394>.
- Escárcega, R.O., Fuentes-Alexandro, S., García-Carrasco, M., Gatica, A., Zamora, A., 2007. The transcription factor nuclear factor-kappa B and cancer. *Clin. Oncol.* 19 (2), 154–161. <https://doi.org/10.1016/j.clon.2006.11.013>.
- Fang, Y., Eglén, R.M., 2017. Three-dimensional cell cultures in drug discovery and development. *SLAS Discovery* 22 (5), 456–472. <https://doi.org/10.1177/1087057117696795>.
- Gullo, L., Mazzaracchio, V., Colozza, N., Duranti, L., Fiore, L., Arduini, F., 2024. Carbon black as a cost-effective nanomodifier for (electro)chemical-free pre-treatment thermoplastic polyurethane-based 3D printed electrodes. *Electrochim. Acta* 482, 143982. <https://doi.org/10.1016/j.electacta.2024.143982>.
- Han, J.J., 2023. <sc>FDA</sc> Modernization Act 2.0 allows for alternatives to animal testing. *Artif. Organs* 47 (3), 449–450. <https://doi.org/10.1111/aor.14503>.
- Heggstad, J.T., Kinnamon, D.S., Liu, J., Joh, D.Y., Fontes, C.M., Wei, Q., Ozcan, A., Hucknall, A.M., Chilkoti, A., 2022. Smartphone enabled point-of-care detection of serum biomarkers, 343–365. https://doi.org/10.1007/978-1-0716-1803-5_19.
- Jensen, C., Teng, Y., 2020. Is it time to start transitioning from 2D to 3D cell culture? *Front. Mol. Biosci.* 7 <https://doi.org/10.3389/fmolb.2020.00033>.
- Kosheleva, N.V., Efremov, Y.M., Shavkuta, B.S., Zurina, I.M., Zhang, D., Zhang, Y., Minaev, N.V., Gorkun, A.A., Wei, S., Shpichka, A.I., Saburina, I.N., Timashev, P.S., 2020. Cell spheroid fusion: beyond liquid drops model. *Sci. Rep.* 10 (1), 12614 <https://doi.org/10.1038/s41598-020-69540-8>.
- Lambrechts, D., Roeffaers, M., Goossens, K., Hofkens, J., Van de Putte, T., Schrooten, J., Van Oosterwyck, H., 2014. A causal relation between bioluminescence and oxygen to quantify the cell niche. *PLoS One* 9 (5), e97572. <https://doi.org/10.1371/journal.pone.0097572>.
- Langhans, S.A., 2018. Three-dimensional in vitro cell culture models in drug discovery and drug repositioning. *Front. Pharmacol.* 9 <https://doi.org/10.3389/fphar.2018.00006>.
- Li, D., Huang, Q., Lu, M., Zhang, L., Yang, Z., Zong, M., Tao, L., 2015. The organophosphate insecticide chlorpyrifos confers its genotoxic effects by inducing DNA damage and cell apoptosis. *Chemosphere* 135, 387–393. <https://doi.org/10.1016/j.chemosphere.2015.05.024>.
- Moehling, T.J., Lee, D.H., Henderson, M.E., McDonald, M.K., Tsang, P.H., Kaakeh, S., Kim, E.S., Woreley, S.T., Kinzer-Ursem, T.L., Clayton, K.N., Linnes, J.C., 2020. A smartphone-based particle diffusometry platform for sub-attomolar detection of *Vibrio cholerae* in environmental water. *Biosens. Bioelectron.* 167, 112497 <https://doi.org/10.1016/j.bios.2020.112497>.
- Nath, P., Mahtaba, K.R., Ray, A., 2023. Fluorescence-based portable assays for detection of biological and chemical analytes. *Sensors* 23 (11), 5053. <https://doi.org/10.3390/s23115053>.
- Nowak, P.M., Wietecha-Posuszny, R., Pawliszyn, J., 2021. White analytical chemistry: an approach to reconcile the principles of green analytical chemistry and functionality. *TrAC, Trends Anal. Chem.* 138, 116223 <https://doi.org/10.1016/j.trac.2021.116223>.
- Schenone, M., Dančák, V., Wagner, B.K., Clemons, P.A., 2013. Target identification and mechanism of action in chemical biology and drug discovery. *Nat. Chem. Biol.* 9 (4), 232–240. <https://doi.org/10.1038/nchembio.1199>.
- Schramm, S., Weiß, D., 2024. Bioluminescence – the vibrant glow of nature and its chemical mechanisms. *Chembiochem.* <https://doi.org/10.1002/cbic.202400106>.
- Vakhshiteh, F., Bagheri, Z., Soleimani, M., Ahvaraki, A., Pourmemat, P., Alavi, S.E., Madjd, Z., 2023. Heterotypic tumor spheroids: a platform for nanomedicine evaluation. *J. Nanobiotechnol.* 21 (1), 249. <https://doi.org/10.1186/s12951-023-02021-y>.
- Wlodkowic, D., Jansen, M., 2022. High-throughput screening paradigms in ecotoxicity testing: emerging prospects and ongoing challenges. *Chemosphere* 307, 135929. <https://doi.org/10.1016/j.chemosphere.2022.135929>.
- Yao, Z., Zhang, B.S., Prescher, J.A., 2018. Advances in bioluminescence imaging: new probes from old recipes. *Curr. Opin. Chem. Biol.* 45, 148–156. <https://doi.org/10.1016/j.cbpa.2018.05.009>.
- Zeinhom, M.M.A., Wang, Y., Song, Y., Zhu, M.-J., Lin, Y., Du, D., 2018. A portable smartphone device for rapid and sensitive detection of *E. coli* O157:H7 in Yoghurt and Egg. *Biosens. Bioelectron.* 99, 479–485. <https://doi.org/10.1016/j.bios.2017.08.002>.
- Żuchowska, A., Baranowska, P., Flont, M., Brzózka, Z., Jastrzębska, E., 2024. Review: 3D cell models for organ-on-a-chip applications. *Anal. Chim. Acta* 1301, 342413. <https://doi.org/10.1016/j.ajca.2024.342413>.